

# Separation of Elastic Waves in Split Hopkinson Bars Using One-point Strain Measurements

by S. W. Park and M. Zhou

**ABSTRACT**—A method for the analysis of elastic waves in split Hopkinson bars for unlimited time durations is presented. This method allows the separation of component waves traveling in opposite directions in each bar using the strain history measured at one point on the bar and a known end condition for it. The method extends the time period for which valid experimental data can be extracted for a split Hopkinson bar apparatus and eliminates the need for a second independent measurement of the stress waves required in other methods for such extended analyses. Comparisons with the two-point method, which requires two independent strain measurements, show good agreement between the two methods. The accuracy and feasibility of the method are demonstrated through its application to impact experiments on composite laminates. The use of the current method in determining the response of a fiber-reinforced composite laminate under impact loading is described.

**KEY WORDS**—elastic waves, SHPB, one-point method, impact, fiber-reinforced composites

The technique of a split Hopkinson pressure bar (SHPB) has been widely used in studies of the dynamic behavior of materials. This wide use is largely due to its ability to resolve the time evolution of material response and the simplicity of its operation. The technique is based on the theoretical analysis of wave motion in the elastic bars involved. Following the original introduction by Hopkinson<sup>1</sup> and an extensive critical study by Davies,<sup>2</sup> Kolsky<sup>3</sup> developed the present form of split bars with the specimen being sandwiched in between. Over the years, the technique has been extended to tensile<sup>4</sup> and torsional<sup>5</sup> configurations.

In the analysis of SHPB measurements, the time duration for direct interpretation of incident, reflected and transmitted pulses from strain gage readings is usually possible for only up to the time of one round-trip wave reflection in the bars. The lengths of bars and the positions of strain gages are designed such that the incident pulse and the first reflected pulse in each bar can be recorded separately during this period. Subsequently, the superposition of stress pulses traveling in opposite directions complicates strain gage readings and makes the direct inference of individual pulses difficult. As a result, measurements outside this time window are usually discarded, and the corresponding portion of material response remains unanalyzed.

---

*S. W. Park is a Research Scientist, and M. Zhou is an Assistant Professor, George W. Woodruff School of Mechanical Engineering, Georgia Institute of Technology, Atlanta, GA 30332-0405.*

*Original manuscript submitted: June 22, 1998.  
Final manuscript received: May 17, 1999.*

However, there are cases in which the extended time history of mechanical quantities is needed. For instance, when testing low-impedance materials, such as the polymeric foam analyzed by Zhao and Gary,<sup>6</sup> the desired maximum strain is large. Therefore, longer test duration and longer measurements are needed. Bacon, Farm and Lataillade<sup>7</sup> studied dynamic fracture toughness of brittle materials based on the extended time histories of force and load-point displacement measured using a modified Hopkinson pressure bar. The analysis of the impact response of composite laminates is another example. Damage in the specimen often accumulates over an extended period of time due to repeated impact of the incident bar on the specimen. Although it is often desirable to use experimental configurations that impart only one loading pulse on the specimen,<sup>8,9</sup> multiple incident pulses simulate actual contact interactions in certain applications and provide an opportunity for the damage evolution in the specimen material to be analyzed. Such an analysis necessitates interpretation of the time history of damage evolution through the histories of contact force, displacement and energy absorption for the duration of interest beyond the initial period of one round-trip wave propagation in the bars.

Lundberg and Henchoz<sup>10</sup> presented a recursive formula for determining the extended histories of strain, normal force and particle velocity from the strain histories measured at two different locations on a bar. This method (referred to as the two-point method) is based on the theory of one-dimensional wave propagation in cylindrical bars and involves solving time domain difference equations. The method was used by Karlsson, Lundberg and Sundin<sup>11</sup> to investigate the interaction between a drill bit and rock in percussive drilling and by Lundberg, Carlsson and Sundin<sup>12</sup> to analyze the wave propagation in a nonuniform bar with a variable characteristic impedance. Yanagihara<sup>13</sup> independently proposed the two-point method with a similar numerical formulation as given by Lundberg and Henchoz.<sup>10</sup> Recently, Zhao and Gary<sup>6</sup> improved the two-point method by incorporating a correction for dispersion effects and applied the method to the testing of polymeric foams and metallic tubes that involve large strains and displacements.

In the two-point method, two independent strain histories must be measured to determine the unknown functions for the two transient pulses traveling in opposite directions in a bar. However, most SHPB apparatuses involve one gage on the input bar and one gage on the output bar. Also, they are designed such that at least one end condition (usually traction free) of each bar is known at all times. These facts can be used

to eliminate one of the measurements needed in the two-point method.

In this paper, we will show that the two unknown wave functions can be determined from one measured strain history and a known end condition. A new algorithm for the separation of the two component wave functions is presented below. Referred to as the one-point method hereafter, this method allows the conventional SHPB configuration to be used without any modification. Another benefit is that a large amount of existing data acquired from a one-gage setup can be reanalyzed for extended material response characterization. The accuracy of this method is demonstrated through its application to impact experiments on a fiber-reinforced composite laminate. A comparison is also given between the new method and the two-point method.

### Separation of Elastic Waves in the SHPB

Wave motion in a slender cylindrical bar can be described by the one-dimensional wave equation

$$\frac{\partial^2 u}{\partial x^2} = \frac{1}{c^2} \frac{\partial^2 u}{\partial t^2}, \quad (1)$$

where  $c = (E/\rho)^{.5}$  is the longitudinal wave speed of the bar, with  $E$  being the Young's modulus and  $\rho$  the mass density of the bar material. The general solution to (1) consists of two arbitrary functions that represent the wave forms traveling in the positive and negative  $x$ -directions, that is,

$$u(x, t) = u_1 \left( t - \frac{x}{c} \right) + u_2 \left( t + \frac{x}{c} \right). \quad (2)$$

The longitudinal strain may be expressed in a similar form:

$$\varepsilon(x, t) = \varepsilon_1 \left( t - \frac{x}{c} \right) + \varepsilon_2 \left( t + \frac{x}{c} \right), \quad (3)$$

where  $\varepsilon(x, t) = \partial u(x, t)/\partial x$  and functions  $\varepsilon_1$  and  $\varepsilon_2$  are related to  $u_1$  and  $u_2$  by  $c\varepsilon_1(\xi) = -du_1(\xi)/d\xi$  and  $c\varepsilon_2(\eta) = du_2(\eta)/d\eta$ , respectively. The particle velocity can be written, in terms of  $\varepsilon_1$  and  $\varepsilon_2$ , as

$$v(x, t) = c \left[ -\varepsilon_1 \left( t - \frac{x}{c} \right) + \varepsilon_2 \left( t + \frac{x}{c} \right) \right], \quad (4)$$

where  $v(x, t) = \partial u(x, t)/\partial t$ . Other mechanical quantities, such as stress, mechanical power and strain energy density, can be determined from the strain and velocity given by (3) and (4). Clearly, the complete solution depends entirely on functions  $\varepsilon_1$  and  $\varepsilon_2$ . Therefore, an essential part of the analysis is to determine these functions using strain measurements.

Figure 1 is a schematic illustration of a typical SHPB apparatus. The specimen is placed between the input and output bars. Impact is generated by the striker bar, which is propelled by a gas gun. Usually, one strain gage station is placed on the input bar and another on the output bar. At each gage station, two strain gages are mounted diametrically opposite to each other on the bar to enhance the signal and ignore the bending effect. The strain gage output is recorded by a high-speed oscilloscope during the experiment.

In the two-point method, as summarized in the appendix,  $\varepsilon_1$  and  $\varepsilon_2$  are determined through direct measurement of strain histories at two different locations on each of the bars. This approach requires an additional gage to be mounted on each of the bars. In a typical SHPB test, the left end of the input bar is free of traction at all times except for the duration when it is in contact with the striker bar. For the output bar, the right end of the bar is free of traction at all times until it is arrested by a stopper long after the experiment. In both cases, the strain history at the free end is zero. This known condition can be used effectively to replace one of the measurements needed in the two-point method.

Figure 2 shows the Lagrangian (or time-distance) diagram for wave propagation in a cylindrical bar of length  $L$ . The strain gage is mounted at a distance  $a$  from the left end. The right-going wave is  $\varepsilon_1$ , and the left-going wave is  $\varepsilon_2$ . Substitution of  $x = a$  into (3) results in

$$\varepsilon_A(t) = \varepsilon_1(t - t_a) + \varepsilon_2(t + t_a), \quad (5)$$

where  $\varepsilon_A(t) = \varepsilon(a, t)$  and  $t_a = a/c$ . The input and output bars are considered separately because of the difference in their end conditions.

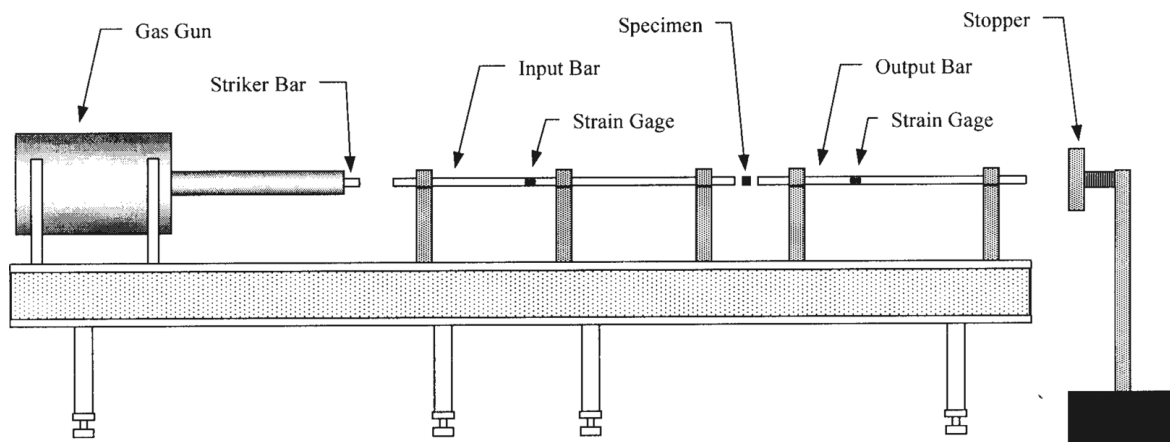


Fig. 1—A schematic illustration of the split Hopkinson pressure bar apparatus



and

$$\varepsilon_2(\eta) = \begin{cases} 0 & \text{for } \eta < T, \\ -\varepsilon_1(\eta - T) & \text{for } \eta > T. \end{cases} \quad (17)$$

### Experimental Verification and Application of the Method

#### Verification Using an Experiment on Composites

To verify its accuracy, the one-point method is used to analyze the wave propagation during a three-point bend impact experiment. The configuration of the experiment is shown in Fig. 3. The specimen (76.2 mm × 19.05 mm × 3.78 mm), made of a 16-ply, quasi-isotropic, S-2 glass/BMI composite laminate, is placed between the input and output bars via a miniature three-point bend fixture. This fixture facilitates localized damage in the specimen under impact loading. The impact response of the specimen over an extended period of time is analyzed. Specifically, the histories of contact force, displacement and mechanical work are determined using the one-point method. Two strain gages are mounted on each bar as shown in Fig. 3, providing two independent measurements in each case. Only one gage on each bar (e.g., A for the input bar and C for the output bar) is needed for the one-point method. The second gage (B and D for the two bars, respectively) is used to provide a redundant measure to validate the calculated results at the same location using the one-point method.

Figure 4 shows the strain histories measured by gages A and C. The initial compressive wave is partly reflected back into the input bar as a tensile wave by the input bar-specimen interface and partly transmitted into the output bar through the specimen as a compressive wave. A series of bar-specimen interactions and free-end reflections continue following initial impact. Wave functions  $\varepsilon_1$  and  $\varepsilon_2$  are determined using (12)-(13) for the input bar and (16)-(17) for the output bar. The results are shown in Fig. 5. Note that  $\xi = t - t_a$  and  $\eta = t + t_a$ , as previously defined. The functions

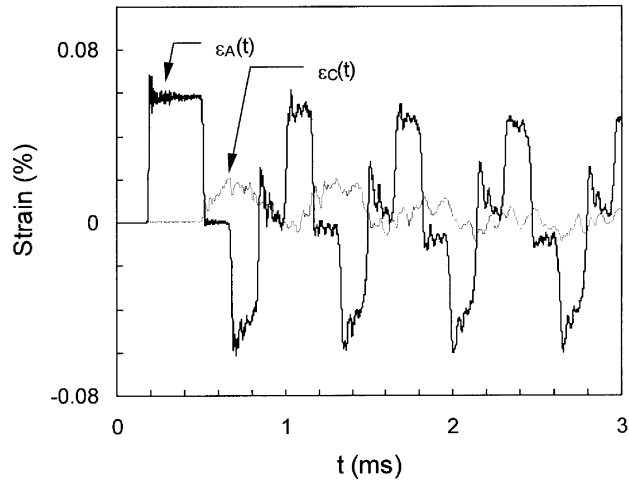
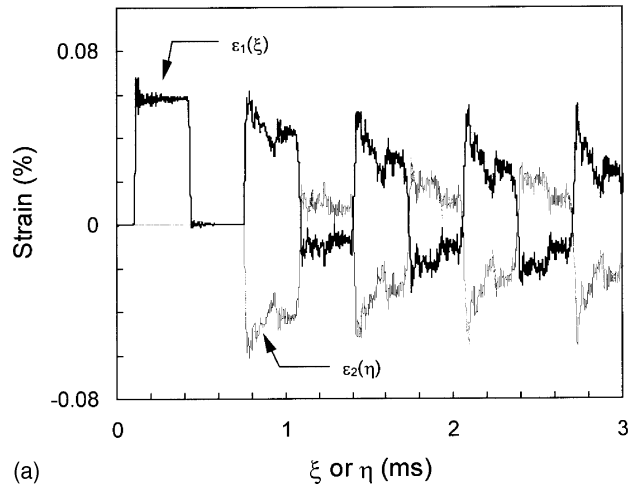
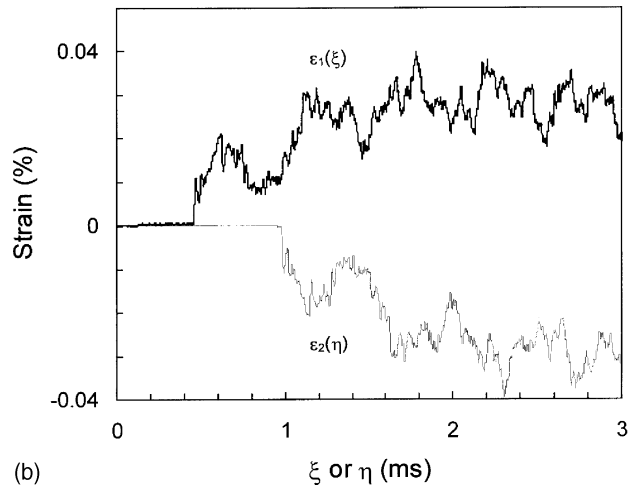


Fig. 4—Strain histories measured at A and C



(a)



(b)

Fig. 5—Wave functions  $\varepsilon_1$  and  $\varepsilon_2$ : (a) input bar, (b) output bar

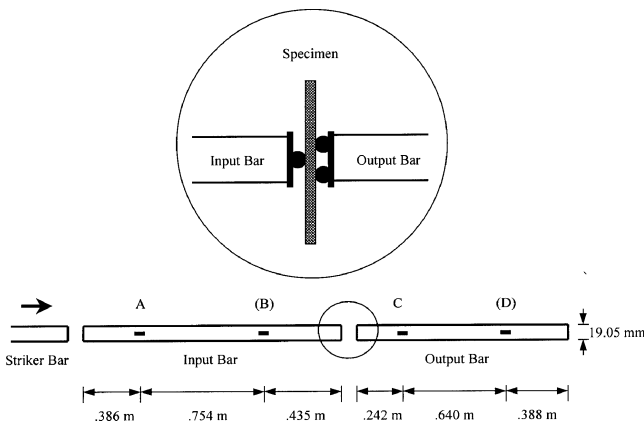
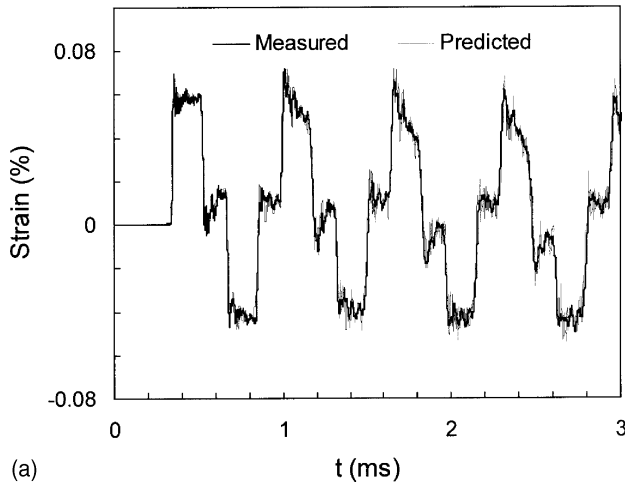
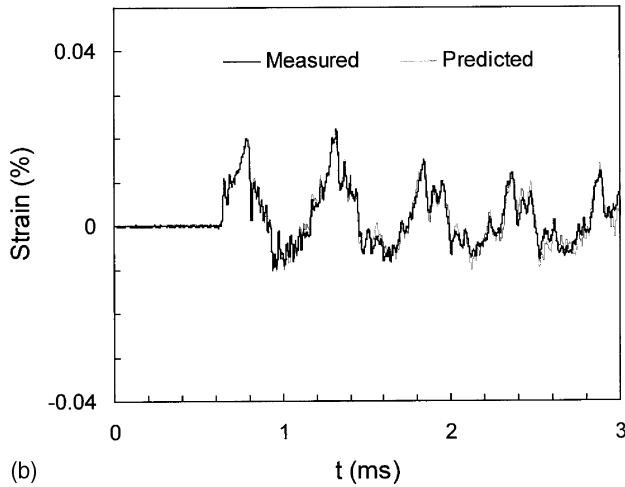


Fig. 3—Configuration of an impact experiment on a composite laminate

allow the strain histories at B and D to be calculated via (3). A comparison of the calculated profiles and the measured profiles is given in Fig. 6. Good agreement is seen for the input and output bars. The small local differences can be attributed to the effects of dispersion and signal noise.



(a)



(b)

Fig. 6—A comparison of measured and predicted strain histories (a) at B, (b) at D

To further validate the proposed method and compare it with the two-point method, experiments were conducted using the striker and the input bar only. It was found that the one-point method and the two-point method predict the waveforms equally well.

### Impact Response of a Composite Laminate

Particular attention is given to contact force history, particle velocity, displacement, work transfer and energy absorption during the impact loading. The normal forces at the input bar-specimen and specimen-output bar interfaces are computed via

$$\begin{aligned} F_{in}(t) &= AE\varepsilon_{in}(L, t) \\ F_{out}(t) &= AE\varepsilon_{out}(0, t), \end{aligned} \quad (18)$$

where  $A$  is the cross-sectional area of the bars and  $\varepsilon_{in}$  and  $\varepsilon_{out}$  denote strains in the input and output bars, respectively. Figure 7 shows  $F_{out}(t)$  obtained using (18). In the

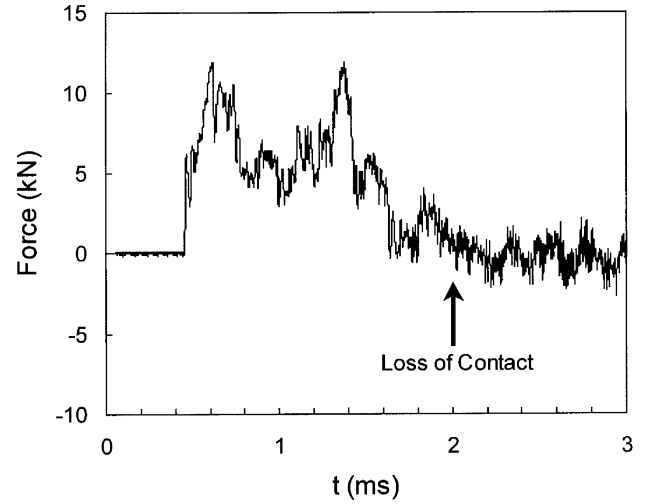


Fig. 7—Contact force history at the specimen-output bar interface

experiments conducted, the forces on the two sides of the specimen are essentially the same except for small experimental noise. Clearly, compressive loading on the specimen occurs primarily during the first two cycles of wave reverberation in the input bar, and bar-specimen interaction ceases after approximately 2 ms.

The velocity histories at the interfaces are computed via (4). Here,  $x = L$  for the input bar-specimen interface, and  $x = 0$  for the specimen-output bar interface. These profiles are plotted in Fig. 8. It can be seen that the velocity at the input bar end gradually becomes oscillatory and the output bar end gradually picks up speed during the experiment.

The histories of mechanical power through the two interfaces are calculated from the force and velocity histories at the interfaces. The work done by the input bar to the specimen is

$$W_{in}(t) = \int_0^t P_{in}(t) dt = AE \int_0^t \varepsilon_{in}(L, t) v_{in}(L, t) dt. \quad (19)$$

Similarly, the work done by the specimen to the output bar is

$$W_{out}(t) = \int_0^t P_{out}(t) dt = AE \int_0^t \varepsilon_{out}(0, t) v_{out}(0, t) dt \quad (20)$$

In (19) and (20),  $P$  is mechanical power and  $v_{in}$  and  $v_{out}$  are particle velocities in the input and output bars, respectively. The energy absorbed by the specimen is the difference between  $W_{in}$  and  $W_{out}$ , that is,

$$E_{abs}(t) = W_{in}(t) - W_{out}(t). \quad (21)$$

The histories of  $W_{in}$ ,  $W_{out}$  and  $E_{abs}$  are shown in Fig. 9. Note that the energy absorbed by the specimen has a recoverable part and an unrecoverable part. The unrecoverable part of the energy is expended on generating damage. The fluctuations in the absorbed energy profile in Fig. 9 are due to the storage and release of strain energy during the impact process. This figure indicates that most of the energy absorption occurs during the first two cycles of wave reverberation (up to 2 ms, consistent with the contact force history in Fig. 7).

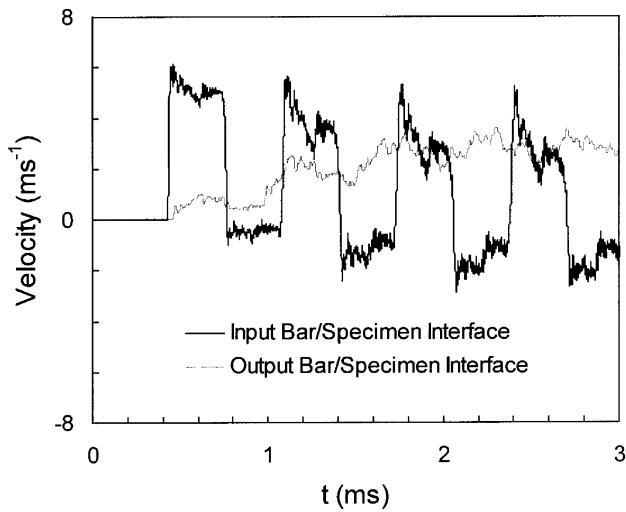


Fig. 8—Velocity histories at the bar-specimen interfaces

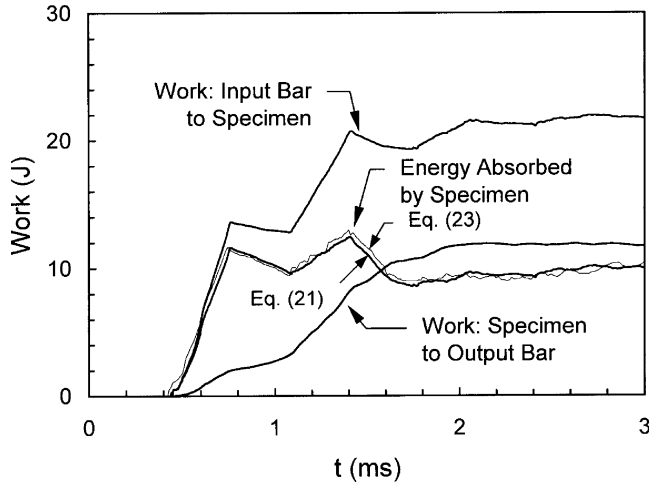


Fig. 9—Work histories at the bar-specimen interfaces

The work transfer between the bars and the specimen can also be calculated by keeping track of the energy in the input and output bars, thus providing a cross-check for the energy absorbency calculation. The total energy in an elastic bar of length  $L$  at any given time  $t$  is

$$E(t) = E_k(t) + E_p(t) = \int_0^L \frac{1}{2} A \rho v^2(x, t) dx + \int_0^L \frac{1}{2} A E \varepsilon^2(x, t) dx, \quad (22)$$

where  $E_k$  and  $E_p$  denote the kinetic and strain energies, respectively. The distributions of  $v$  and  $\varepsilon$  at an arbitrary time of  $t = 3$  ms for the input and output bars are shown in Figs. 10(a) and 10(b), respectively. The energy absorbed by the specimen during impact is given by

$$E_{abs}(t) = E_{input} - E_{in}(t) - E_{out}(t), \quad (23)$$

where  $E_{input}$  is the total energy input into the system and  $E_{in}$  and  $E_{out}$  are the energy carried by the input and output bars, respectively. The total energy input into the system is the kinetic energy of the striker bar at  $t = 0$  which may also be

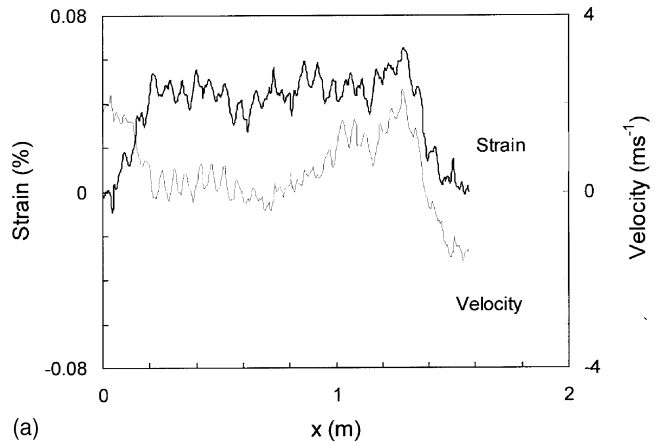
calculated from the initial rectangular waveform measured from gage A (see Fig. 4), that is,

$$E_{input} = \frac{1}{2} \rho A L_0 V_0^2 = \int_{t_a}^{t_a + \Delta t} A E c \varepsilon_A^2(t) dt, \quad (24)$$

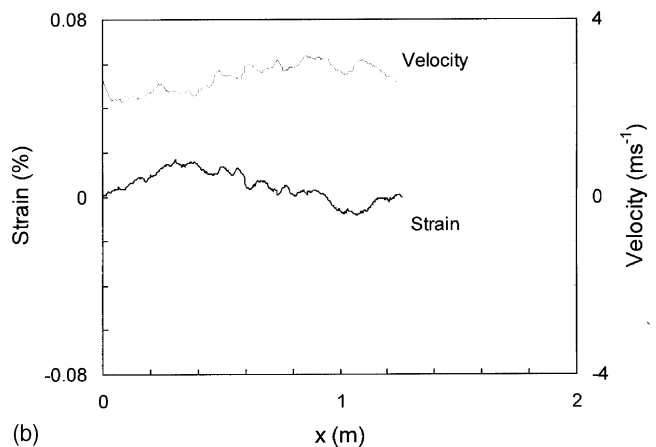
where  $t_a$  is the time of arrival of the wave front at gage A and  $\Delta t = 2L_0/c$  is the duration of the initial rectangular waveform. Note that  $E_k = E_p$  in this case. The energy absorbed by the specimen calculated according to (23) is also shown in Fig. 9. The calculations essentially match those from (21). It should be pointed out that the energy absorbed by the three-point bend fixture is estimated to be very small and negligible. Specifically, the total energy carried by the fixture (with a mass of 0.05 kg) is less than 0.1 J.

### Effect of Dispersion

The treatment of wave propagation based on (1) as discussed above assumes that the pulse shapes remain unchanged as they propagate (i.e., *nondispersive*). However, this assumption is valid only when the impact that produces the pulse is applied slowly. Otherwise, the resulting pulse shows dispersion.<sup>2</sup> According to the Pochhammer frequency equation,<sup>14</sup> phase velocity is a decreasing function of frequency (or wave number) of the harmonic wave components and dispersion is more significant for long wavelengths.



(a)



(b)

Fig. 10—Distributions of strain and velocity at  $t = 3$  ms: (a) input bar, (b) output bar

A number of authors have analyzed the dispersion effect and corrections for it in the SHPB.<sup>15–18</sup> They have shown that dispersion correction can enhance the analysis accuracy, especially when the diameter of the bar is large. However, in most cases, the dispersion corrections were limited to the incident, first reflected or transmitted pulses. Recently, Zhao and Gary<sup>6</sup> incorporated a dispersion correction scheme into the two-point method and applied the scheme to the analysis of SHPB tests for extended durations. This scheme may also be incorporated into the one-point method. However, as Zhao and Gary pointed out, dispersion correction for a waveform stretched over an extended period of time is difficult, and correction can be made only in an approximate sense. For example, when the analysis time window stretches over an extended duration, the waveforms of  $\varepsilon_1$  and  $\varepsilon_2$ , obtained either from the one-point method or the two-point method, are long and highly irregular in general. In this case, dispersion corrections on a segment-by-segment basis may be considered. A lengthy waveform is first segmented into a number of waveforms, each of which is defined only over a finite time interval (and set to be zero outside this interval). Each segment is dispersion corrected on an individual basis. However, it is found that Fourier transform of segmented waveforms often produces waveforms containing sharp (vertical) peaks and valleys, and hence dispersion correction in this case is not very useful. Because of the numerical difficulties encountered, and because the diameter (19.05 mm) of the bars involved in our tests is not particularly large, no dispersion correction is incorporated in our current analysis. However, in principle, one may incorporate dispersion correction (at least on a segment-by-segment basis) into the one-point method presented in this paper.

## Conclusions

A simple, efficient algorithm for separating component waves traveling in opposite directions in cylindrical, elastic bars is presented and validated experimentally. The algorithm is based on the one-dimensional wave propagation theory and requires the use of measured strain history at only one location on a bar and a known end condition for it. Application of this algorithm requires that the striker bar be shorter than the input bar less the distance between the strain gage station and the striker-input bar interface, a condition trivially satisfied in most SHPB configurations. The method, like the existing two-point method, effectively eliminates the limit on the time window for valid data interpretation in the conventional SHPB technique. The validity of the method is verified experimentally by comparing predictions and direct measurements. While obviating the need for one of the experimental measurements in the two-point method, the new method has the same accuracy as that of the two-point method. The one-point method allows the conventional SHPB configuration to be used without any modification for the analysis of material behavior over an unlimited duration of time. An additional benefit is that a large amount of existing data acquired from one-gage SHPB setups can be reanalyzed for extended material response characterization. This new method is used to analyze the impact response of a fiber-reinforced polymer-matrix composite in a three-point bend loading configuration. The histories of contact force, boundary velocities, mechanical work and absorbed energy are obtained.

## Appendix: The Two-Point Method

The algorithm using two strain measurements was originally presented by Lundberg and Henchoz<sup>10</sup> and Yanagihara.<sup>13</sup> This method is recast here in a manner consistent with the one-point method for comparison of the two methods.

The strain histories at point A ( $x = a$ ) and point B ( $x = b$ ) on a bar can be written via (3) as

$$\varepsilon_A(t) = \varepsilon_1(t - t_a) + \varepsilon_2(t + t_a) \quad (\text{A1})$$

and

$$\varepsilon_B(t) = \varepsilon_1(t - t_b) + \varepsilon_2(t + t_b), \quad (\text{A2})$$

where  $\varepsilon_A(t) = \varepsilon(a, t)$ ,  $\varepsilon_B(t) = \varepsilon(b, t)$ ,  $t_a = a/c$  and  $t_b = b/c$ .

(a) FOR  $t < T - t_a$  (WHERE  $T = 2L/c$ ; SEE FIG. 2)

No reflected wave passes at  $x = a$ , thus,

$$\varepsilon_2(t + t_a) = 0. \quad (\text{A3})$$

From (A1) and (A3), one finds

$$\varepsilon_A(t) = \varepsilon_1(t - t_a). \quad (\text{A4})$$

Information from  $\varepsilon_B(t)$  is redundant and unused for this period of time.

(b) FOR  $t > T - t_a$

Equation (A2) can be transformed, with an appropriate shift in time, into

$$\varepsilon_B(t - t_b + t_a) = \varepsilon_1(t - 2t_b + t_a) + \varepsilon_2(t + t_a). \quad (\text{A5})$$

Subtracting (A5) from (A1) and rearranging, one finds

$$\varepsilon_1(t - t_a) = \varepsilon_1(t - 2t_b + t_a) + \varepsilon_A(t) - \varepsilon_B(t - t_b + t_a). \quad (\text{A6})$$

From (A1), one finds

$$\varepsilon_2(t + t_a) = -\varepsilon_1(t - t_a) + \varepsilon_A(t). \quad (\text{A7})$$

(A3), (A4), (A6) and (A7) can be combined, with changes of variables,  $(t - t_a) \rightarrow \xi$  and  $(t + t_a) \rightarrow \eta$ , to yield functions  $\varepsilon_1$  and  $\varepsilon_2$  for the bar in terms of  $\varepsilon_A$  and  $\varepsilon_B$  as

$$\varepsilon_1(\xi) = \begin{cases} \varepsilon_A(\xi + t_a) & \text{for } \xi < T - 2t_a \\ \varepsilon_1(\xi - 2t_b + 2t_a) \\ \quad + \varepsilon_A(\xi + t_a) & \\ -\varepsilon_B(\xi - t_b + 2t_a) & \text{for } \xi > T - 2t_a \end{cases} \quad (\text{A8})$$

and

$$\varepsilon_2(\eta) = \begin{cases} 0 & \text{for } \eta < T. \\ -\varepsilon_1(\eta - 2t_a) + \varepsilon_A(\eta - t_a) & \text{for } \eta > T \end{cases} \quad (\text{A9})$$

It should be noted that in contrast to the one-point method, no end condition is involved here; therefore, there is no specific restriction on the duration of input pulse applied by the striker bar.

## Acknowledgment

Support from the Office of Naval Research (Scientific Officer Yapa D.S. Rajapaske) is gratefully acknowledged.

## References

1. Hopkinson, B., "A Method of Measuring the Pressure in the Deformation of High Explosives or by the Impact of Bullets," *Phil. Trans. Royal Soc.*, **A213**, 437–452 (1914).
2. Davies, R.M., "A Critical Study of the Hopkinson Pressure Bar," *Phil. Trans. Royal Soc. London*, **A240**, 375–457 (1948).
3. Kolsky, H., "An Investigation of the Mechanical Properties of Materials at Very High Rates of Loading," *Proc. Phys. Soc.*, **B62**, 676–700 (1949).
4. Harding, J., Wood, E.D., and Campbell, J.D., "Tensile Testing of Material at Impact Rates of Strain," *J. Mech. Eng. Sci.*, **2**, 88–96 (1960).
5. Baker, W.W. and Yew, C.H., "Strain Rate Effects in the Propagation of Torsional Plastic Waves," *J. Appl. Mech.*, **33**, 917–923 (1966).
6. Zhao, H. and Gary, G., "A New Method for the Separation of Waves: Application to the SHPB Technique for an Unlimited Duration of Measurement," *J. Mech. Phys. Solids*, **45**, 1185–1202 (1997).
7. Bacon, C., Farm, J., and Lataillade, J.L., "Dynamic Fracture Toughness Determined from Load-point Displacement," *EXPERIMENTAL MECHANICS*, **34**, 217–223 (1994).
8. Nemat-Nasser, S., Isaacs, J.B., and Starrett, J.E., "Hopkinson Techniques for Dynamic Recovery Experiments," *Proc. Royal Soc. London*, **A435**, 371–391 (1991).
9. Chen, W. and Ravichandran, G., "Dynamic Compressive Failure of a Glass-ceramic under Lateral Confinement," *J. Mech. Phys. Solids*, **45**, 1303–1328 (1997).
10. Lundberg, B. and Henchoz, A., "Analysis of Elastic Waves from Two-point Strain Measurement," *EXPERIMENTAL MECHANICS*, **17** (6), 213–218 (1977).
11. Karlsson, L.G., Lundberg, B., and Sundin, K.G., "Experimental Study of a Percussive Process for Rock Fragmentation," *Int. J. Rock Mech. Min. Sci. Geomech. Abstracts*, **26**, 45–50 (1989).
12. Lundberg, B., Carlsson, J., and Sundin, K.G., "Analysis of Elastic Waves in Non-uniform Rods from Two-point Strain Measurement," *J. Sound Vibration*, **137**, 483–493 (1990).
13. Yanagihara, N., "New Measuring Method of Impact Force," *Bull. Jap. Soc. Mech. Engineers*, **21**, 1085–1088 (1978).
14. Achenbach, J.D., *Wave Propagation in Elastic Solids*, North-Holland, Amsterdam (1975).
15. Follansbee, P.S. and Frantz, C., "Wave Propagation in the Split Hopkinson Pressure Bar," *J. Eng. Mat. Tech.*, **105**, 61–66 (1983).
16. Gong, J.C., Malvern, L.E., and Jenkins, D.A., "Dispersion Investigation in the Split Hopkinson Pressure Bar," *J. Eng. Mat. Tech.*, **112**, 309–314 (1990).
17. Lifshitz, J.M. and Leber, H., "Data Processing in the Split Hopkinson Pressure Bar Tests," *Int. J. Impact Eng.*, **15**, 723–733 (1994).
18. Zhao, H. and Gary, G., "On the Use of SHPB Techniques to Determine the Dynamic Behavior of Materials in the Range of Small Strains," *Int. J. Solids Struct.*, **33** (23), 3363–3375 (1996).